CHEMISTRY OF MATERIALS
Article

Chem. Mater. **2009,** *21,* 3871–3882 3871
DOI:10.1021/cm9012156

Synthesis, Mesomorphism, and Luminescent Properties of Calamitic 2-Phenylpyridines and Their Complexes with Platinum(II)

Amedeo Santoro,[†] Adrian C. Whitwood,[†] J. A. Gareth Williams,[‡] Valery N. Kozhevnikov,*[,†] and Duncan W. Bruce*[,†]

[†]*Department of Chemistry, University of York, Heslington, York YO10 5DD, U.K., and* [‡]*Department of Chemistry, University of Durham, University Science Laboratories, South Road, Durham DH1 3LE, U.K.*

Received May 3, 2009. Revised Manuscript Received June 23, 2009

The liquid crystal and luminescent properties of two related series of rod-like, ortho-platinated complexes bearing a β-diketonate co-ligand are reported. The parent ligands exhibit a rich, smectic polymorphism, but when modified with a fused cyclopentene ring, nematic phases dominate. Reaction of the ligands with tetrachloroplatinate(II) leads to poorly soluble, dimeric complexes that can be cleaved using dimethylsulfoxide; the resulting monomeric complexes are then readily converted to the β-diketonate complexes. All of the complexes are mesomorphic, and the β-diketonate complexes have excited state lifetimes of 27 μs with emission quantum efficiencies exceeding 0.5, the highest yet reported for materials of this type.

Introduction

Molecular materials for various optoelectronic applications occupy a special place in materials chemistry research as there exist several examples of real, and highly profitable, applications. In each case, improvements in device performance can be linked to, among other things, the tuning of bulk properties via molecular design so that an intimate knowledge of structure/function relationships is a key factor in determining advances. There are several different device types where charge transport or luminescence is one of the key properties, for example in OLEDs (organic light-emitting diodes), TFTs (thin-film transistors), organic solar cells, active components for image and data treatment and storage, solid organic lasers, and photovoltaic devices.[1] In all of these systems, liquid-crystalline order, namely, an organized, supramolecular structure, could be expected to improve charge mobility due to the cooperativity of physical properties in these self-organized materials.[2] Thus, combining liquid crystals with one or more other, desirable properties leads to the need for multifunctional materials where, for example, light emission may be found in a mesomorphic material.

A large series of emissive nonmetal liquid crystals are nowadays under intense investigation for their application in the OLED devices,[3] and one of the main classes of LCs for device application are the liquid crystalline polymers and oligomers[3b,3c] showing very high photoluminescence efficiency and improved current−voltage characteristics.

With regard to emissive materials, transition-metal complexes have been featured strongly in recent years as they can allow access both to singlet and triplet manifolds, greatly improving the efficiency of potential devices.[4] In this regard, 2-phenylpyridine complexes of iridium(III) have been particularly well studied,[5] along with 2-phenylpyridine complexes of platinum(II)[6] and, more recently, 1,3-*bis*-(2-pyridyl)benzene complexes of platinum(II).[7,8] Combining the properties of these efficient emitters with liquid crystallinity is a valuable target as the emissive properties of the complex core can be combined with the order and fluidity possible through the liquid crystal state. Thus, while there are several examples

*Corresponding authors. Fax: (+44) 1904 432516. E-mail: db519@york.ac.uk; vk503@york.ac.uk.

(1) (a) Laschat, S.; Baro, A.; Steinke, N.; Giesselmann, F.; Hägele, C.; Scalia, G.; Judele, R.; Kapatsina, E.; Sauer, S.; Schreivogel, A.; Tosoni, M. *Angew. Chem., Int. Ed.* **2007**, *46*, 4832. (b) Xiao, S.; Myers, M.; Miao, Q.; Sanaur, S.; Pang, K.; Steigerwald, M. L.; Nuckolls, C. *Angew. Chem., Int. Ed.* **2005**, *44*, 7390. (c) Nelson, J. *Science* **2001**, *293*, 1059. (d) Schmidt-Mende, L.; Fechtenkötter, A.; Müllen, K.; Moons, E.; Friend, R. H.; Mackenzie, J. D. *Science* **2001**, *293*, 1119. (e) Forrest, S. R. *Nature* **2004**, *428*, 911.
(2) O'Neill, M.; Kelly, S. M. *Adv. Mater.* **2003**, *15*, 1135.
(3) (a) Gimenez, R.; Pinol, M.; Serrano, J. L. *Chem. Mater.* **2004**, *16*, 1377. (b) Aldred, M. P.; Eastwood, A. J.; Kelly, S. M.; Vlachos, P.; Contoret, A. E. A.; Farrar, S. R.; Mansoor, B.; O'Neil, M.; Tsoi, W. C. *Chem. Mater.* **2004**, *16*, 4928. (c) Aldred, M. P.; Contoret, A. E. A.; Farrar, S. R.; Kelly, S. M.; Mathieson, D.; O'Neill, M.; Tsoi, W. C.; Vlachos, P. *Adv. Mater.* **2005**, *17*, 1368. (d) Zhang, X. L.; Yamaguchi, R.; Moriyama, K.; Kadowaki, M.; Kobayashi, T.; Ishi-i, T.; Thiemann, T.; Mataka, S. *J. Mater. Chem.* **2006**, *16*, 736. (e) Sagara, Y.; Kato, T. *Angew. Chem., Int. Ed.* **2008**, *47*, 5175. (f) Sagara, Y.; Yamane, S.; Mutai, T.; Araki, K.; Kato, T. *Adv. Funct. Mater.* **2009**, *19*, 1869.
(4) Evans, R. C.; Douglas, P.; Winscom, C. J. *Coord. Chem. Rev.* **2006**, *250*, 2093.
(5) Lowry, M. S.; Bernhard, S. *Chem.—Eur. J.* **2006**, *12*, 7970.
(6) Brooks, J.; Babayan, Y.; Lamansky, S.; Djurovich, P. I.; Tsyba, I.; Bau, R.; Thompson, M. E. *Inorg. Chem.* **2002**, *41*, 3055.
(7) (a) Williams, J. A. G.; Beeby, A.; Davies, E. S.; Weinstein, J. A.; Wilson, C. *Inorg. Chem.* **2003**, *42*, 8609. (b) Cocchi, M.; Virgili, D.; Fattori, V.; Rochester, D. L.; Williams, J. A. G. *Adv. Funct. Mater.* **2007**, *17*, 285. (c) Virgili, D.; Cocchi, M.; Fattori, V.; Satatini, C.; Kalinowski, J.; Williams, J. A. G. *Chem. Phys. Lett.* **2006**, *433*, 145. (d) Cocchi, M.; Kalinowski, J.; Virgili, D.; Fattori, V.; Develay, S.; Williams, J. A. G. *Appl. Phys. Lett.* **2007**, *90*, 163508.
(8) Kozhevnikov, V. N.; Donnio, B.; Bruce, D. W. *Angew. Chem., Int. Ed.* **2008**, *47*, 6286.

Published on Web 08/04/2009

Scheme 1. Preparation of the 2,6-Di(4-alkoxyphenyl)pyridine Ligands[a]

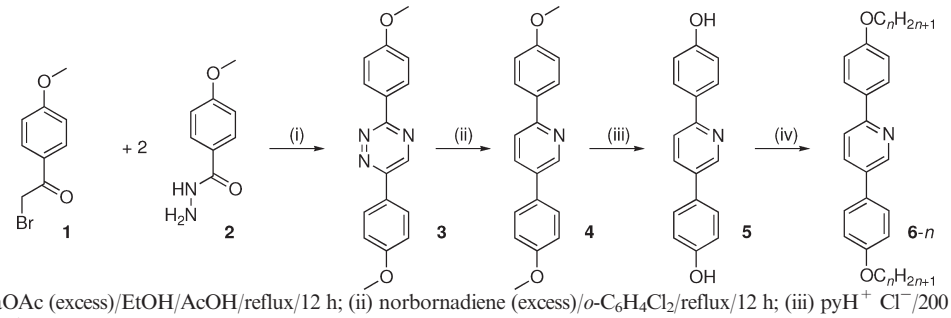

[a] Conditions: (i) NaOAc (excess)/EtOH/AcOH/reflux/12 h; (ii) norbornadiene (excess)/*o*-$C_6H_4Cl_2$/reflux/12 h; (iii) pyH^+ Cl^-/200 °C/12 h; (iv) C_nH_{2n+1}Br/DMF/base/90 °C 12 h.

of emissive metallomesogens,[9,10] only three reports deal with mesomorphic derivatives of the luminescent Pt^{II} systems, and while there are reports of amphiphilic Ir^{III} systems, none has an LC phase.[11]

Thus, Venkatesan et al. reported a series of Pt^{II} complexes of substituted 2-phenyl- and 2-thienyl-pyridines, containing a hexasubstituted diphenyl-1,3-diketonato ligand. The materials exhibited columnar mesophases with the liquid crystallinity being driven by the attendant hexasubstituted β-diketonate, although two less substituted examples were found to show a SmA phase. Emission wavelengths could be tuned from 494 to 576 nm, with excited state lifetimes between 0.5 and 11 μs. On the other hand, Thomas et al.[12b] reported poorer emission efficiencies for Pt^{II} complexes with diphenyl-1,3-diketonato, as opposed to acetylacetonate, due to the increased mixing with the CT state. Damm et al.[13] reported the luminescent and the liquid crystal properties of a series of ortho-metalated 2-phenylpyrimidines, although no data for quantum yield and lifetimes were given. More recently, we reported on the preparation of liquid-crystalline derivatives of the platinum(II) complexes of a 1,3-*bis*-(2-pyridyl)benzene complex where we were able to show that the liquid crystal state provided access to a form of organization that led to emission from the monomeric complex, rather than an excimer or aggregate.[8]

The preparation of the 1,3-bis-(2-pyridyl)benzene ligands used in this latter study employed a very flexible chemistry for *N*-heterocycle synthesis, which first involves the formation of a hydrozone oxime followed by its condensation with an aldehyde to give a triazine. Use of an inverse electron demand Diels−Alder procedure (for example, using norbornadiene) eliminates dinitrogen and leads to the related pyridine. This chemistry has been employed in the preparation of a number of functional materials,[14] including calamitic liquid crystals.[15]

Employing this chemistry, two series of calamitic 2,5-diphenylpyridine ligands have been prepared in the present work, one of which has the pyridine fused with a cyclopentene ring. The fused ring is expected to moderate transition temperatures and favor the nematic phase, while in addition steric effects were also found (vide infra). These materials have then been complexed to platinum(II) to give dichloro-bridged dinuclear complexes which, on bridge cleavage, led subsequently to emissive dmso and acac complexes. The preparation, liquid crystal and optical properties of these materials are described.

Synthesis

The key to the preparation of the ligands (Scheme 1) is the first step, which uses a methodology described by Saraswathi and Srinivasan in the early 1970s[16] where 2-bromoacetophenone (**1**) reacts with 2 equiv of 4-methoxybenzohydrazide (**2**) in the presence of base to give 3,6-bis(4-methoxyphenyl)-1,2,4-triazine (**3**). The remainder of the preparation uses well-defined chemistry so that the triazine reacts with norbornadiene to give pyridine **4**, which is then demethylated to the diphenol (**5**) using molten pyridinium chloride and finally realkylated (Williamson ether conditions) to give the product, **6**-*n* (*n* refers to the number of carbon atoms in the terminal alkoxy chains).

To obtain the related compound with the fused cyclopentene ring (**8**-*n*), the retro Diels−Alder reaction is carried out (Scheme 2) with 1-(*N*-morpholino)cyclopentene to give pyridine **7**, after which the product is again obtained by demethylation/alkylation.

(9) (a) Bayón, R.; Coco, S.; Espinet, P. *Chem.—Eur. J.* **2005**, *11*, 1079. (b) Suàrez, S.; Mamula, O.; Imbert, D.; Piguet, C.; Bunzli, J. -C. G. *Chem. Commun.* **2003**, 1226. (c) Cardinaels, T.; Driesen, K.; Parac-Vogt, T. N.; Heinrich, B.; Bourgogne, C.; Guillon, D.; Donnio, B.; Binnemans, K. *Chem. Mater.* **2005**, *17*, 6589. (d) Barberio, G.; Bellusci, A.; Crispini, A.; Donnio, B.; Giorgini, L.; Ghedini, M.; La Deda, M.; Pucci, D.; Szerb, E. I. *Chem.—Eur. J.* **2006**, *12*, 6738.
(10) For a short review, see: Binnemans, K. *J. Mater. Chem.* **2009**, *19*, 448.
(11) (a) Guerrero-Martinez, A.; Vida, Y.; Dominguez-Gutierrez, D.; Albuquerque, R. Q.; de Cola, L. *Inorg. Chem.* **2008**, *47*, 9131. (b) Neve, F.; La Deda, M.; Crispini, A.; Bellusci, A.; Puntoriero, F.; Campagna, S. *Organometallics* **2004**, *23*, 5856.
(12) (a) Venkatesan, K.; Kouwer, P. H. J.; Yagi, S.; Müller, P.; Swager, T. M. *J. Mater. Chem.* **2008**, *18*, 400. (b) Thomas, S. W.; Yagi, S.; Swager, T. M. *J. Mater. Chem.* **2005**, *15*, 2829.
(13) Damm, C.; Israel, G.; Hegmann, T.; Tschierske, C. *J. Mater. Chem.* **2006**, *16*, 1808.
(14) (a) Kozhevnikov, V. N.; Ustinova, M. M.; Slepukhin, P. A.; Santoro, A.; Bruce, D. W.; Kozhevnikov, D. N. *Tetrahedron. Lett.* **2008**, *49*, 4096. (b) Kozhevnikov, V. N.; Kozhevnikov, D. N.; Shabunina, O. V.; Rusinov, V. L.; Chupakhin, O. N. *Tetrahedron Lett.* **2005**, *46*, 1791. (c) Kozhevnikov, V. N.; Kozhevnikov, D. N.; Shabunina, O. V.; Rusinov, V. L.; Chupakhin, O. N. *Tetrah. Lett.* **2005**, *46*, 1521. (d) Kozhevnikov, V. N.; Kozhevnikov, D. N.; Nikitina, T. V.; Rusinov, V. L.; Chupakhin, O. N.; Zabel, M.; König, B. *J. Org. Chem.* **2003**, *68*, 2882. (e) Kozhevnikov, D. N.; Kozhevnikov, V. N.; Ustinova, M. M.; Santoro, A.; Bruce, D. W.; Koenig, B.; Czerwieniec, R.; Fischer, T.; Zabel, M.; Yersin, H. *Inorg. Chem.* **2009**, *48*, 4179.
(15) Kozhevnikov, V. N.; Cowling, S. C.; Karadakov, P. B.; Bruce, D. W. *J. Mater. Chem.* **2008**, *18*, 1703.
(16) Saraswathi, T. V.; Srinivasan, V. R. *Tetrahedron Lett.* **1971**, *12*, 2315.

Scheme 2. Preparation of the 2,6-Di(4-alkoxyphenyl)pyridine Ligands Bearing a Fused Cyclopentene Group[a]

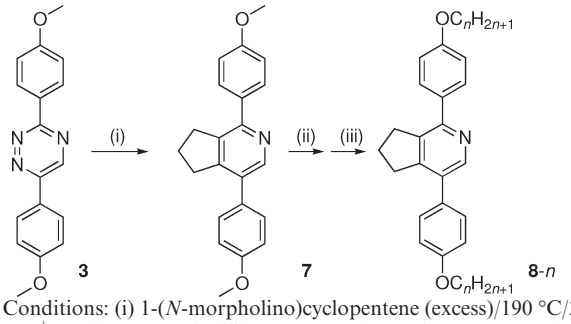

[a] Conditions: (i) 1-(*N*-morpholino)cyclopentene (excess)/190 °C/3 h; (ii) $pyH^+ Cl^-$/200 °C/12 h; (iii) $C_nH_{2n+1}Br$/DMF/base/90 °C 12 h.

Once these ligands were prepared, they were reacted with $K_2[PtCl_4]$ in wet AcOH to give the dichloro-bridged dimers in moderate yield (Scheme 3). The solubility of these dimers was extremely low, and no useful spectroscopic data could be obtained. In fact, this low solubility proved to be a problem as subsequent direct reaction with Na(acac) proceeded either not at all or in very low yield. However, this situation could be improved greatly if the dimers were first reacted with dmso under reflux for 30 min, which led to bridge cleavage and to soluble mononuclear complexes containing dmso as one of the ligands. These products (**11**-*n*) were obtained in very good yield after purification *via* a short silica column and could then be reacted with $Na(acac)\cdot H_2O$ in acetone to give the target β-diketonate complexes. Analogous chemistry led to the related complexes of diphenylpyridines (**12**-*n* and **14**-*n*) with a fused cyclopentene ring (Scheme 3). The complexes were characterized inter alia by ^1H NMR spectroscopy, where resolved couplings between ^1H and ^{195}Pt were observed. Polarization transfer experiments were used to confirm that the dmso complexes existed as the isomer where the coordinated dmso was found trans to the pyridine nitrogen. Details of these experiments are found in the Supporting Information.

Crystal and Molecular Structure of 12-6, 13-6, and 14-6

To investigate these new complexes further, single crystals were grown for examples of three of the four families of complexes, namely, **12**-6, **13**-6, and **14**-6. Despite repeated efforts, however, we could not obtain good quality crystals of a derivative of the series **11**-*n*. Basic crystallographic data are collected in Table 1, while cif files are available with the Supporting Information.

For complex **13**-6, there are two molecules in the unit cell (Figure 1). One gives a slightly bowed appearance when viewed side-on, while the other appears somewhat more planar. Curiously, in the molecule that is generally more bowed, the central part containing the bound phenylpyridine, platinum, and the acac ligand appears rather close to planar, whereas in the less bowed molecule, the acac ligand is moved slightly out of that plane. In both cases, however, the Pt atoms are located *in* the plane of the four binding ligands (maximum deviation 0.022(1) Å). Around the Pt centers, there is little difference between the two unique complexes, for example, the two O−Pt−O angles are 92.64(10) and 92.62(9)°, while the two C−Pt−N angles are 82.18(13) and 81.86(13)°. Consistent with the higher trans influence of C with respect to N, the Pt−O distances trans to carbon are longer (2.081(2) Å) than the distances where Pt−O is trans to N (2.001(2) Å). The high trans influence of the carbon ligand has been noted previously.[6,17] The Pt−Pt separation is 7.195 Å.

In complex **14**-6, the pyridine ring is modified by having a fused cyclopentene ring attached, which is clearly seen in Figure 2. There is one molecule in the unit cell, and a side-on view (Supporting Information) shows that the entire complex is almost planar (Pt deviates from complete planarity by 0.01(1) Å) save for the twisting out of plane of the unbound phenyl ring attached to the pyridine, 22.50(12)°, and a buckling of the fused cyclopentene ring by about 10° at the apical CH_2 group. The C−Pt−N angle is slightly tighter at 81.01(9)° than that found in **13**-6, and the same is true for the O−Pt−O angle at 91.51(7)°. Pt−O trans to carbon is again longer (2.0855(17) Å) than that trans to nitrogen (2.0067(16) Å). The shortest Pt−Pt separation is 7.151 Å, although the packing of the complexes shows some evidence of $\pi-\pi$ stacking, with an inter-ring separation of some 3.45 Å.

The crystal structure of **12**-6, on the other hand, is much more complicated, and the asymmetric unit contained six molecules of the complex (labeled A−F). For this reason, the data now referred to are collected in tables in the Supporting Information; the molecular structure of one of these complexes is shown as Figure 3. The central portions of these complexes are essentially the same; the binding atoms (C_1, N_1, Cl_1, S_1) are coplanar, with the platinum being positioned about 0.1 Å out of this plane (Supporting Information). There is also little variation in metal−ligand distances and ligand−metal−ligand angles between the complexes (Supporting Information). The pyridyl and binding phenyl (C_1-C_6) rings are coplanar with a maximum deviation of 2.66° in molecule A (Supporting Information) and also lie in the plane of the chlorine and sulfur.

However, there are two main differences between the structures of the complexes. These are the angle between the second phenyl and the pyridyl ring, which varies from 35.78(17)° to 47.05(17)° (Supporting Information), and the conformation of the hexyl chains. For the latter, only 3 of the 12 chains exhibit the staggered, all-*trans* arrangement ($C_{27B}-C_{32B}$, $C_{21D}-C_{26D}$, $C_{21F}-C_{26F}$), whereas all the other hexyl chains exhibit different conformations with three of the chains exhibiting disorder (molecules A, B, and D); in each case, the disorder was modeled over two positions.

The intermolecular arrangement of the complexes exhibits some interesting behavior. The central, planar parts of the complexes lie parallel to each other in a layered arrangement. The complexes are organized in pairs (A and F, B and C, D and E), the molecules in each pair

(17) Ghedini, M.; Pucci, D.; Crispini, A.; Barberio, G. *Organometallics* **1999**, *18*, 2116.

Scheme 3. Preparation of the Platinum−dmso and Platinum−acac Complexes of the Diphenylpyridine Ligands[a]

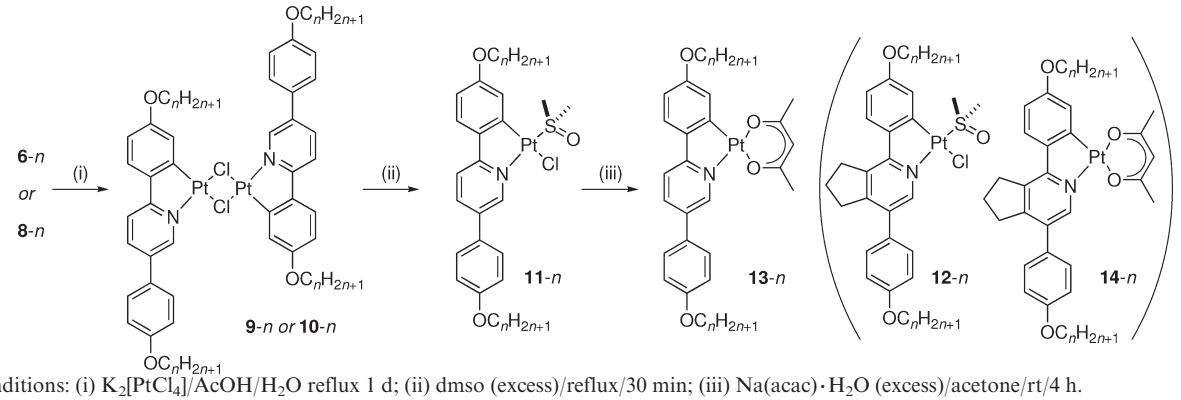

[a] Conditions: (i) $K_2[PtCl_4]$/AcOH/H_2O reflux 1 d; (ii) dmso (excess)/reflux/30 min; (iii) Na(acac)·H_2O (excess)/acetone/rt/4 h.

Table 1. Crystallographic Data for Complexes 12-6, 13-6, and 14-6

	12-6	**13**-6	**14**-6
CCDC deposition number	729975	729976	729977
empirical formula	$C_{34}H_{46}ClNO_3PtS$	$C_{34}H_{43}NO_4Pt$	$C_{37}H_{47}NO_4Pt$
formula weight, g mol^{-1}	779.32	724.78	764.85
T, K	110(2)	110(2)	110(2)
λ, Å	0.71073	0.71073	0.71073
crystal system	monoclinic	triclinic	triclinic
space group	$P2(1)/n$	$P\bar{1}$	$P\bar{1}$
unit cell dimensions, Å	a = 25.5055(12)	a = 11.6719(6)	a = 11.5266(7)
	b = 21.3004(10)	b = 13.2121(7)	b = 11.5631(7)
	c = 37.4088(18)	c = 20.8465(11)	c = 13.0188(8)
unit cell angles, deg	α = 90	α = 72.9600(10)	α = 102.9400(10)
	β = 108.1210(10)	β = 80.7870(10)	β = 90.9280(10)
	γ = 90	γ = 86.4890(10)	γ = 109.1230(10)
volume, Å^3	19315.3(16)	3033.6(3)	1590.23(17)
Z	24	4	2
ρ_{calcd}, Mg m^{-3}	1.608	1.587	1.597
absorption coefficient, mm^{-1}	4.541	4.663	4.453
F(000)	9408	1456	772
crystal size, mm^3	0.22 × 0.21 × 0.15	0.14 × 0.14 × 0.12	0.24 × 0.21 × 0.06
θ range for data collection	0.86 to 28.30	1.77 to 28.30	1.61 to 30.03
index ranges	$-33 \le h \le 33$, $-28 \le h \le 28$, $-49 \le h \le 49$	$-15 \le h \le 15$, $-17 \le h \le 17$, $-27 \le h \le 27$	$-15 \le h \le 15$, $-16 \le h \le 16$, $-18 \le h \le 18$
reflections collected	198312	31669	17935
independent reflections	47979 [R_{int} = 0.0387]	14932 [R_{int} = 0.0195]	8907 [R_{int} = 0.0190]
Completeness	99.9% (θ = 28.30°)	98.9% (θ = 28.30°)	95.7 (θ = 30.03°)
absorption correction	semiempirical from equivalents	semiempirical from equivalents	semiempirical from equivalents
max and min transmission	0.506 and 0.350	0.571 and 0.474	0.766 and 0.428
refinement method	full-matrix least-squares: F^2	full-matrix least-squares: F^2	full-matrix least-squares: F^2
data/restraints/parameters	47979/34/2325	14932/0/730	8907/0/392
goodness-of-fit on F^2	1.080	1.044	1.056
final R indices [$I > 2\sigma I$]	R_1 = 0.0329, wR_2 = 0.0719	R_1 = 0.0284, wR_2 = 0.0695	R_1 = 0.0228, wR_2 = 0.0539
R indices (all data)	R_1 = 0.0491, wR_2 = 0.0790	R_1 = 0.0346, wR_2 = 0.0721	R_1 = 0.0274, wR_2 = 0.0555
largest diff. peak and hole, e Å^{-3}	4.008 and −2.125	6.675 and −0.767	2.210 and −1.127

being related to each other by a 180° rotation approximately parallel to the *b*-axis and midway between the two platinum centers (Figure 4). In each complex pair, the alignment of the planes is such as to minimize the distance between the platinums which can be seen by the $C_1-Pt-Pt$ and $N_1-Pt-Pt$ angles for all pairs being close to 90° (Supporting Information). The alignment between the pairs of complexes is somewhat different with overlap of the 3,4-cyclopentenopyridine rings, although the distance is not significantly less than the sum of the van der Waals radii and so $\pi-\pi$ interactions are relatively unimportant.

Liquid Crystal Properties of the Ligands and Complexes

The diphenylpyridines (**6**-*n*) proved to have a rich mesomorphism, which could be elucidated using polarized optical microscopy; thermal data are collected in Table 2. Having three rings connected only by σ-bonds, it is not surprising that, in general, their melting and clearing points were high, being found from 120 °C (melting point, **6**-10) to 238 °C (clearing point, **6**-6). The richest polymorphic sequence was observed for **6**-6 and is described on cooling from the isotropic phase.

Thus, the first phase seen was a SmA phase, clearly identified by a focal conic fan texture and homeotropic regions. On further cooling this gave way to a SmC phase with a schlieren texture (Figure 5a) where the SmA phase had been homeotropic and broken fans in the planar areas. The SmC phase persisted for some 30 °C, until a transition was observed to a phase that also showed a schlieren texture, but this time the brushes were much broader and ill-defined, and in general, it was

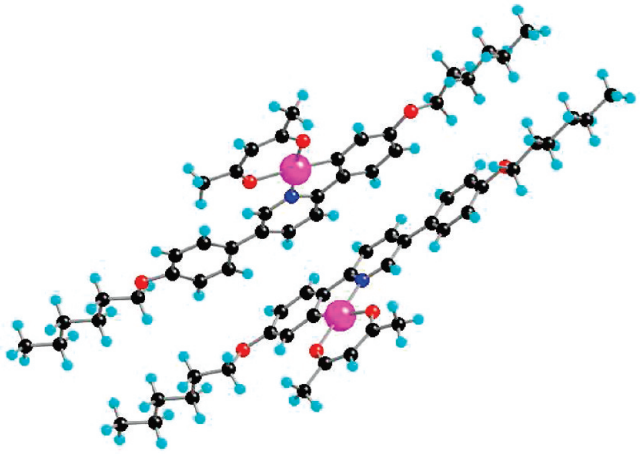

Figure 1. Molecular structure of the two independent molecules in the unit cell of **13**-6.

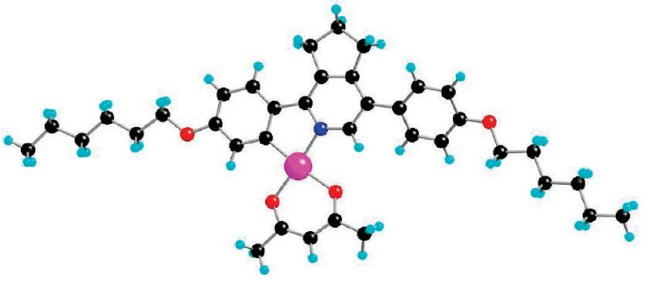

Figure 2. Molecular structure of complex **14**-6.

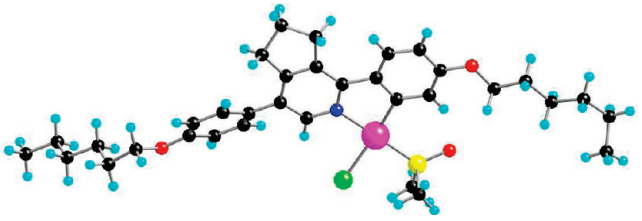

Figure 3. Molecular structure of **12**-6A.

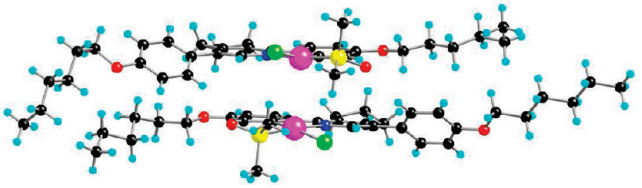

Figure 4. Arrangement of one pair of complexes: **12**-6B and **12**-6C.

difficult to focus well on the sample. This is characteristic of the SmI phase (Figure 5b).[18] This phase persisted for 35 °C before another transition occurred to a fluid phase. Two types of texture could be observed here. One was a classic broken fan texture (Figure 5c) while the other was a sort of mosaic texture (Supporting Information). These are characteristic of a SmF phase. Below the SmF phase, a transition occurred to a crystal smectic phase whose texture (Figure 5d) was consistent with a crystal smectic

(18) Gray, G. W.; Goodby, J. W. *Smectic Liquid Crystals: Textures and Structures*; Leonard Hill: Glasgow, 1984.

Table 2. Thermal Behavior of the Ligands 6-*n* and 8-*n*

compound	transition	T (°C)	ΔH (kJ mol^{-1})	ΔS (J K^{-1} mol^{-1})
6-6	Cr−Cr′	68.8	2.2	6
	Cr'-G	144	1.4	4
	G-SmF	154	8.1	20
	SmF-SmI	166	5.6	13
	SmI-SmC	201.5	1.3	3
	SmC-SmA	231.5	0.3	1
	SmA-I	237.5	8.0	18
6-8	Cr−Cr′[a]	107	10.9	29
	Cr'-J	121	13.4	34
	J-SmI	137	3.8	9
	SmI-SmC	187	2.8	6
	SmC-I	221	13.3	27
6-10	Cr-J[b]	120.3		
	J-SmI	121	41.2[c]	105[c]
	SmI-SmC	178.9	1.4	3
	SmC-I	210.6	14.4	30
6-12	Cr−SmI	121.7	63.0	160
	SmI-SmC	171.6	2.4	5
	SmC-I	200.0	18.5	39
8-6	Cr−N	81.4	29.8	84
	N−I	115.0	1.2	3
8-8	Cr−N	84.8	29.3	82
	N−I	108.7	0.95	3
8-10	Cr−N	99.2	47.8	129
	N−I	105.0	0.6	2
8-12	Cr-SmA	94.8	59.2	161
	SmA-I	101.6	4.8	13

[a] Seen only by DSC. [b] Seen only by microscopy. [c] Combined enthalpy/entropy.

G phase, which would also be the phase predicted to follow a SmF phase on cooling. All of these transitions were identified by DSC analysis, which also showed two transitions between crystal modifications at lower temperatures. The phases and transitions were also seen in the focal conic fan textures, and these photomicrographs are presented in the Supporting Information.

For the longer homologues, the phase behavior changed so that none of **6**-8 to **6**-12 showed a SmA phase, and it was the SmC phase that appeared on cooling the isotropic liquid, once more identified through its characteristic schlieren texture. Cooling again led to formation of a SmI phase, whose range was now some 50 °C in each case, but further cooling led this time directly to the formation of a crystal smectic phase (**6**-8 and **6**-10) or the crystalline phase (**6**-12). Insofar as the crystal smectic phase is concerned, formed from the fluid SmI phase, a crystal smectic J phase would be expected, and for example, we have shown this to be the case previously in extended mesogens.[19] The observed texture (Supporting Information) was also consistent with that of the crystal J phase.

However, when the ligands containing a fused cyclopentene ring were considered, the whole picture was much more straightforward. In general terms, lateral substituents tend to suppress the closer packing required for the formation of smectic phases,[20] and so it was unsurprising to find that **8**-6 to **8**-10 showed only a nematic phase.

(19) Liu, X. -H.; Heinrich, B.; Manners, I.; Guillon, D.; Bruce, D. W. *J. Mater. Chem.* **2000**, *10*, 637.
(20) Weissflog, W. In *Handbook of Liquid Crystals*; Demus, D., Goodby, J., Gray, G. W., Spiess, H.-W., Vill, V., Eds.; Wiley-VCH: Weinheim, 1998; Vol. *2B*, Chapter XI.

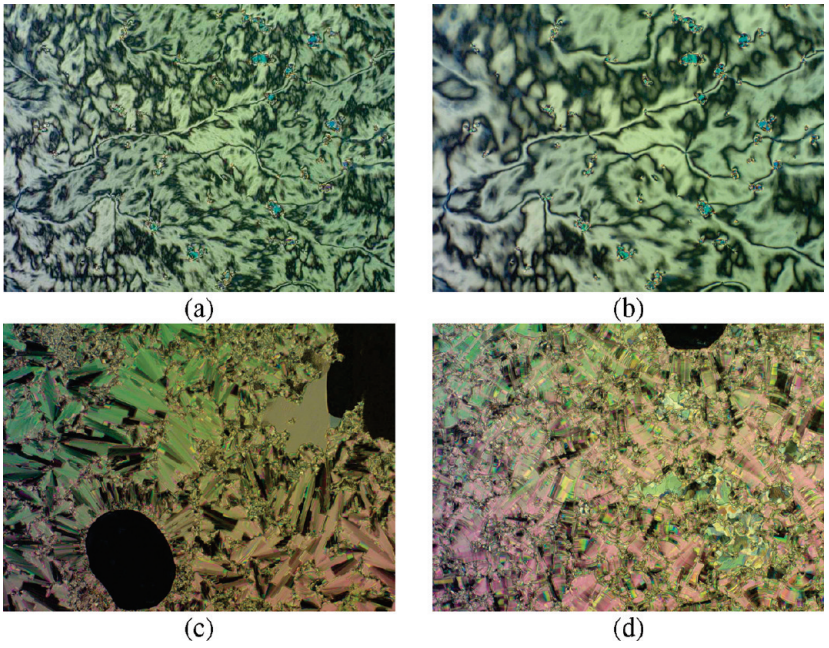

Figure 5. Optical micrographs (on cooling) of the (a) SmC phase at 203 °C; (b) the SmI phase at 198 °C; (c) SmF phase at 159 °C; and (d) crystal smectic G phase at 152 °C.

Table 3. Thermal Behavior of the Platinum Complexes

compound	transition	*T* (°C)	compound	transition	*T* (°C)
13-6	Cr-SmA	200	**14**-10	Cr-I	123
	SmA-I	258		(SmA-I)	115
13-8	Cr-SmA	190	**14**-12	Cr-I	121
	SmA-dec	250		(SmA-I)	119
13-10	Cr-SmA	168	**11**-6	Cr-SmA	200
	SmA-I	244		SmA-I	258
13-12	Cr-SmA	170	**11**-10	Cr-SmA	160
	SmA-I	231		SmA-I	241
14-6	Cr-I	161	**12**-6	Cr-I	198
	(N-I)	101			
14-8	Cr-I	141	**12**-10	Cr-I	138
	(N-I)	(115)		(N-I)	109
	(SmA-N)	(110)			

More than that, the reduction in anisotropy destabilizes both the crystal and the mesophases, and so melting points were in the range 81−99 °C, while clearing points ranged from 105 to 115 °C. The only exception to this behavior was **8**-12, which showed a SmA phase only from 95 to 102 °C, the longer chains allowing the lamellar phase to be stabilized.

The liquid crystal properties of the platinum acac complexes were also simple, and with one exception, none was polymorphic (Table 3). Thus, complexes **13**-*n* derived from ligands **6**-*n* showed only a SmA phase and at temperatures somewhat higher than those of the free ligand. For example, **13**-6 melted at 200 °C and cleared at 258 °C, while **13**-12 melted at 170 °C and cleared at 231 °C. These clearing points are between 20 and 30 °C higher than those of the free ligands, which is in some regards surprising as the Pt(acac) moiety will decrease the structural anisotropy. However, the increased molecular weight and increased polarizability offered by the third-row transition metals[21] will both contribute to the increase. Melting points were at least 50 °C higher than those of the free ligand. Finally, the range of the SmA phase was at least 58 °C in the series and, as expected, both melting point and clearing point decreased with increasing chain length.

For the related complexes (**14**-*n*) prepared from ligands **8**-*n*, it was found that all were monotropic, which was accounted for totally by a stabilization of the crystal phase. For example, in all cases, clearing points were within 20 °C of those of the free ligand, whereas melting points increase by between 24 °C ($n = 10$) and 80 °C ($n = 6$). Complex **14**-6 showed only a nematic phase, while **14**-8 showed both nematic and smectic A; **14**-10 and **14**-12 showed only a SmA phase.

The intermediate dmso complexes were also mesomorphic, and two examples of each were characterized to exemplify their mesomorphism. Thus, **11**-10 showed an enantiotropic SmA phase between 160 and 241 °C, temperatures very similar to those found for the acac complex **13**-10. By comparison, where the ligand possessed the fused ring (**12**-10) a monotropic nematic phase was found at 109 °C below a melting point of 138 °C. Compared to the related acac complex, **14**-10, this represents a small destabilization of the nematic phase and a slightly more significant stabilization of the crystal phase.

Through the comparison between complexes **13**-*n* and the related ligands, **6**-*n*, it is possible to note different aspects of the liquid crystal behavior. The first thing that is clearly visible is the drastic decrease in the number of phases; indeed all complexes **13**-*n* show only a SmA phase while their ligands showed many smectic phases including SmA, SmC, SmF, and SmI as well as crystal G and J phases. This reduction in smectic polymorphism is consistent with much of the literature, in particular as there are no examples of tilted hexagonal phases in

(21) Bertram, C.; Bruce, D. W.; Dunmur, D. A.; Hunt, S. E.; Maitlis, P. M.; McCann, M. *J. Chem. Soc., Chem. Commun.* **1991**, 69.

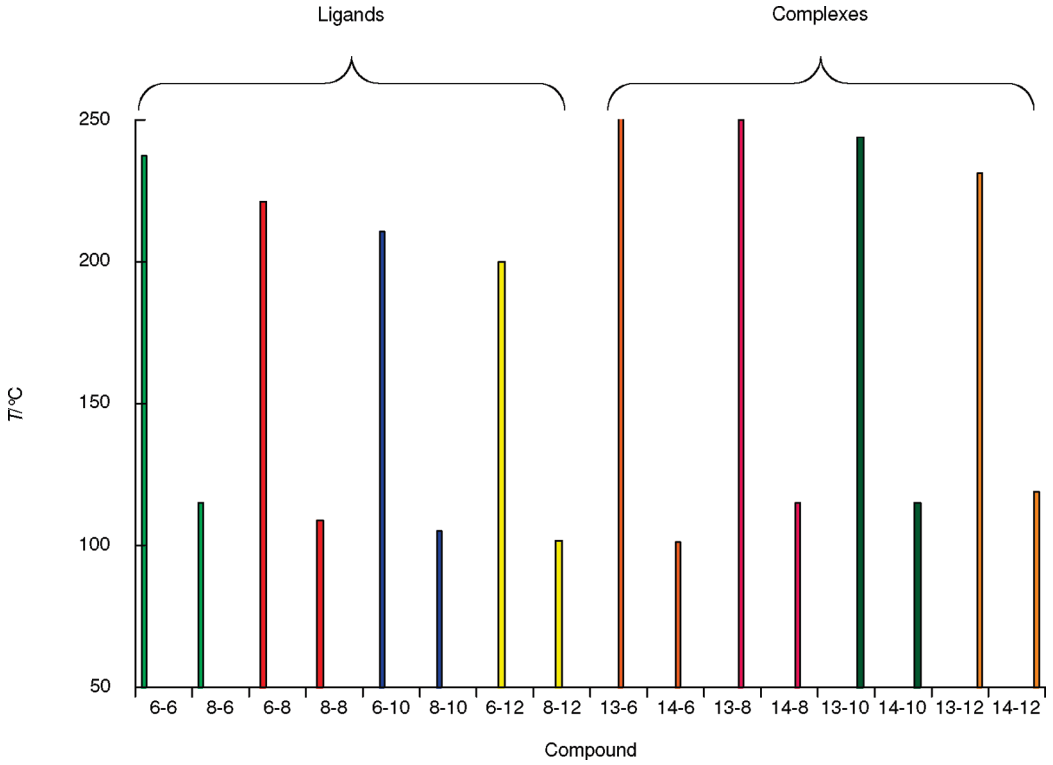

Figure 6. Plot of clearing point as a function of compound for ligands **6**-*n* and **8**-*n* and complexes **13**-*n* and **14**-*n*.

metallomesogens. Another interesting point is the general increase in transition temperatures in complexes **13**-*n* in comparison with the ligand **6**-*n*. Thus, the melting points generally increase on average by 55 °C while the clearing point increases by about 30 °C, an effect ascribed to the larger molecular weight of the metal complexes. Note that for complex **13**-8, it is difficult to determine the temperature of SmA-I transition because the decomposition starts close to the clearing point.

However, what is equally clear with both the ligands and the complexes is that the introduction of the fused cyclopentene ring suppresses polymorphism significantly and also decreases mesophase stability. Figure 6 shows a plot of clearing point as a function of compound type, pairing a ligand and/or its complex with the related material with the fused ring. The mesophase destabilization is obvious, but what is curious is the relative insensitivity of the ligand clearing points to complexation (particularly so for **8**-*n*).

Luminescence Properties of the Complexes

The luminescence properties of the complexes in solution in dichloromethane are discussed first, followed by the behavior in films. All the complexes are emissive in solution at room temperature. The chain length was found to have little influence on the solution luminescence. The C_{12} complexes were selected for more detailed study, for which the solution data are summarized in Table 4 (**13**-12 and **14**-12). Corresponding data for the known complex [Pt(ppy)(acac)] are also included for comparison, together with values for one of the dmso adducts (**11**-6). Representative spectra for **14**-12 are shown in Figure 7.

13-12 and 14-12. The lowest-energy absorption maximum is red-shifted compared to the [Pt(ppy)(acac)] value in both cases. A more pronounced red-shift is observed in emission, but the effect is smaller for the fused-ring complex **14**-12 than for **13**-12: the emission maxima at 298 K are 523 and 541 nm, respectively, compared to 485 nm for [Pt(ppy)(acac)] (Figure 8). The lowering in energy of the emissive state upon introduction of electron-donating alkoxy substituents into the phenyl ring of ppy is anticipated from the destabilization of the HOMO, which is typically localized on the metal and/or cyclometallating ring in such systems. A similar effect was previously observed for the 5-methoxy-substituted complex prepared by Brooks et al.[6] In the present case, the simultaneous introduction of the aryl group into position-5 of the pyridyl ring probably has a more limited effect in destabilizing the LUMO, such that there is a net decrease in the excited state energy and hence a shift to the red. The higher energy of the emissive state of **14**-12 is likely to arise from the steric influence of the *ortho*-CH_2 groups of the cyclopentene ring in disfavoring the planar structure that would maximize conjugation between the rings.

Both complexes are very brightly luminescent, with emission lifetimes at room temperature of 27 μs. The quantum yields at room temperature are around 0.5, considerably superior to that of [Pt(ppy)(acac)]. Indeed, the values are competitive with the brightest Pt-based emitters and appear to be the highest hitherto reported for platinum with ppy-based ligands.[22] Insight into the origin of these high values can be obtained by estimating the

(22) For a review of the luminescence of platinum(II) complexes, see: Williams, J. A. G. *Top. Curr. Chem.* **2007**, *281*, 205.

Table 4. Absorption and Emission Data for Pt Complexes and the Model Compound [Pt(ppy)(acac)], in CH_2Cl_2 at 298 (±3) K except Where Stated Otherwise

	13-12	**14**-12	[Pt(ppy)(acac)]	**11**-6
absorption – λ_{max}, nm (ε, 10^3 M^{-1} cm^{-1})	400 (8.2), 322 (30.5), 305 (24.7), 272 (18.3), 255 (20.4)	400sh (8.9), 386 (10.3), 298 (28.2), 271 (27.1), 256 (25.0)	393sh (2.8), 362 (5.8), 325 (8.8), 312 (9.7), 278 (19.6), 248 (27.2)	397 (12.8), 317 (28.9), 260 (18.7)
emission – λ_{max}, nm	541, 582, 628(sh)	523, 553, 608(sh)	485, 520, 551	550, 588
τ degassed (aerated), μs	27 (0.55)	27 (0.38)	2.6 (0.45)	23 (0.80)
Φ_{lum}	0.49	0.57	0.16	0.08
k_r,[a] 10^4 s^{-1}	1.8	2.1	6.2	0.35
Σk_{nr},[a] 10^4 s^{-1}	1.9	1.6	32	4.0
k_Q,[b] 10^8 $M^{-1}s^{-1}$	8.1	12	8.4	5.5
emission 77 K[c] λ_{max}, nm	526, 562	512, 552, 594	480[d]	532, 574, 616
τ 77 K[c], μs	31	25	9.0[d]	78

[a] k_r and Σk_{nr} are the radiative and nonradiative rate constants estimated on the basis of the luminescence quantum yield and lifetime. [b] Bimolecular rate constant of quenching by molecular oxygen, estimated from lifetimes in degassed and aerated solutions. [c] In ether–isopentane–ethanol (2:2:1). [d] In 2-methyltetrahydrofuran; data from ref 6.

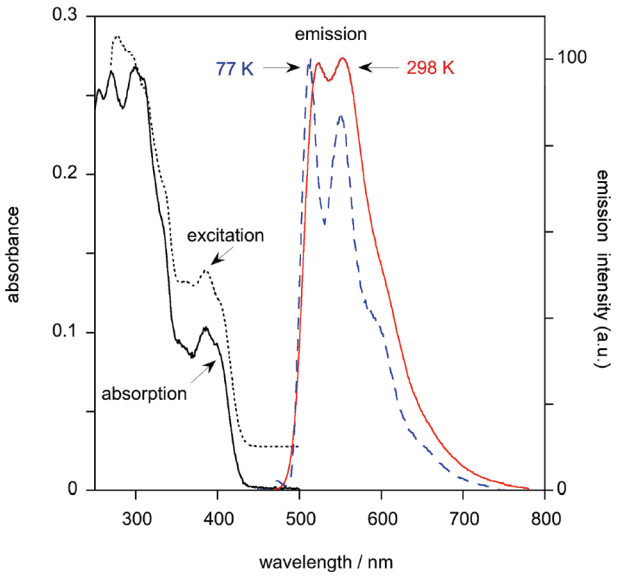

Figure 7. Absorption, excitation (λ_{em} = 545 nm), and emission (λ_{ex} = 400 nm) spectra of **14**-12 in dichloromethane solution at 298 K, and the emission spectrum at 77 K in an ethanol–isopentane–ether glass (2:2:1).

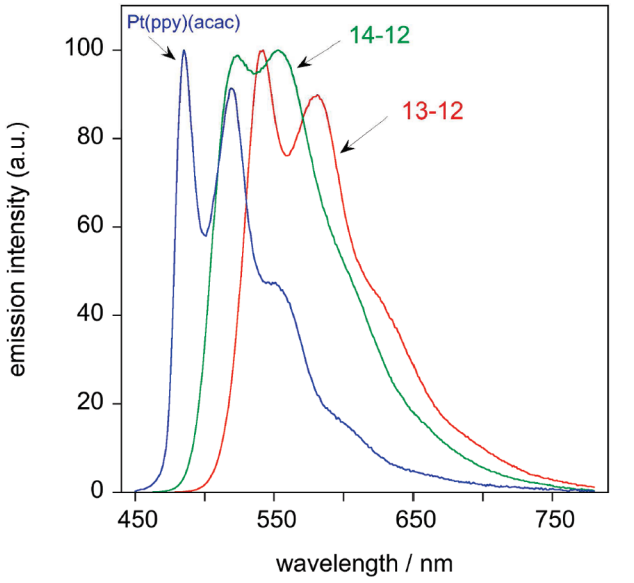

Figure 8. Emission spectra of **13**-12 and **14**-12 in dichloromethane solution at 298 K (λ_{ex} = 400 nm), together with that of [Pt(ppy)(acac)] for comparison.

magnitudes of the radiative and nonradiative rate constants (k_r and Σk_{nr}, respectively) from the lifetimes and quantum yields, as follows:

$$k_r = \Phi_{lum}/\tau \quad \text{and} \quad \Sigma k_{nr} = \tau^{-1} - k_r$$

Although these equations strictly hold only if the emissive state is formed with unitary efficiency, this is likely to be a good approximation, especially given the close match between the excitation and absorption spectra (e.g., Figure 7). Inspection of the data obtained in this way indicates that the improvement in luminescence efficiency relative to [Pt(ppy)(acac)] is due to a large decrease in the sum of the rate constants of the nonradiative decay processes. The platinum complex **13**-1,

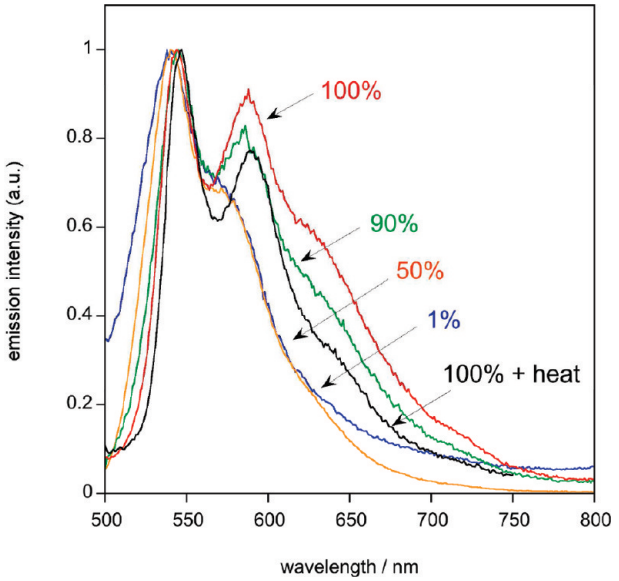

Figure 9. Normalized emission spectra of thin films of **13**-12 in polycarbonate at the proportions by mass indicated. The spectrum of the neat film after heating to 110 °C is also shown.

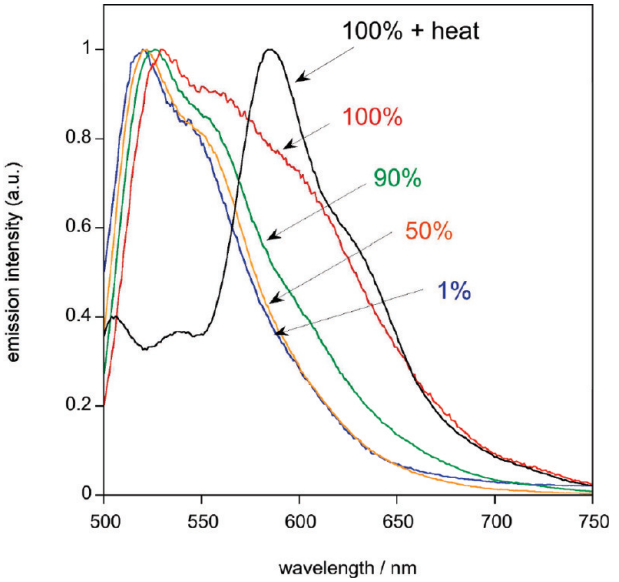

Figure 10. Normalized emission spectra of thin films of **14**-12 in polycarbonate at the proportions by mass indicated, together with the spectrum of the neat film after heating to 110 °C.

incorporating methoxy substituents in place of the long alkoxy chains, shows similarly impressive luminescence characteristics ($\Phi_{lum} = 0.46, \tau = 30\,\mu s$ in CH_2Cl_2 at 298 K; $\tau = 30\,\mu s$ in EPA at 77 K), ruling out the possibility that the reduced nonradiative decay is an effect of the long chains. Most likely, the improvement is associated with the excited state being delocalized over the pendant aryl ring at position 5 of the pyridine atom, rendering it less well coupled to deactivating vibrational modes, such as those associated with the acac ligand. Such an explanation would also account for the somewhat lower radiative decay rates compared to [Pt(ppy)(acac)], as the metal character in the excited state decreases with more extended delocalization over the ligand. There is a slight increase in the ratio of the 0−1 to 0−0 vibrational band intensities on going from 77 to 298 K, which suggests a small change in geometry in the T_1 excited state compared to the ground state. Nevertheless, the observation that the luminescence lifetimes are essentially the same at 77 K as at 298 K is testament to the absence of any significant thermally activated nonradiative decay pathways at ambient temperature.[23]

As expected for complexes with lifetimes of this magnitude, the luminescence is efficiently quenched by oxygen in solution. The bimolecular rate constants for quenching by O_2 are of the order of $10^9\ M^{-1}\ s^{-1}$ (Table 4).

dmso Adducts. The intermediates formed by cleavage of the dimers with dimethylsulfoxide (Scheme 3) are also luminescent, albeit an order of magnitude more weakly so than the acac derivatives. The data in Table 4 suggest that the lower efficiency at room temperature is due primarily to a lower radiative decay rate constant, rather than to elevated nonradiative decay pathways, an explanation which is further supported by the exceptionally long lifetime of 78 μs recorded at 77 K. Possibly the metal orbitals are energetically less well placed for mixing with the π-orbitals of the cyclometallating ligand in the dmso adducts, owing to a more weakly donating set of ancillary ligands.

Luminescence Properties in Films

The luminescence of complexes **13**-12 and **14**-12 was studied at several concentrations within a polycarbonate (PC) host, as thin films prepared by spin coating. In the case of **12**-12, the emission spectrum is unchanged on increasing the concentration from 1% to 50%, but higher concentrations result in a small increase in the relative intensity of the red component of the emission. Normalized spectra are shown in Figures 9 and 10. This enhanced, low-energy emission may be due to the formation of aggregates or excimers, a feature frequently encountered for square planar platinum(II) complexes which can undergo intermolecular face-to-face interactions, for example, through overlap of the d_{z^2} and p_z orbitals orthogonal to the plane of the molecule.[24,25] For example, such species have been used recently to produce white light by extending the emission across the visible region.[26] A similar effect is observed for the cyclopentene-appended complex **13**-12 at high doping levels in PC (Figure 9).

Interestingly, however, a striking difference emerges upon heating the neat (100%) films to 110 °C, close to the melting point of the samples. For example, **14**-12 displays an intense new band at 600 nm at the expense of the emission bands in the 525−550 nm region, whereas the

(23) Williams, J. A. G.; Develay, S.; Rochester, D. L.; Murphy, L. *Coord. Chem. Rev.* **2008**, *252*, 2596.

(24) Houlding, V. H.; Miskowski, V. M. *Coord. Chem. Rev.* **1991**, *111*, 145.

(25) Bailey, J. A.; Hill, M. G.; Marsh, R. E.; Miskowski, V. M.; Schaefer, W. P.; Gray, H. B. *Inorg. Chem.* **1995**, *34*, 4591.

(26) (a) Adamovich, V.; Brooks, J.; Tamayo, A.; Alexander, A. M.; Djurovich, P. I.; D'Andrade, B. W.; Adachi, C.; Forrest, S. R.; Thompson, M. E. *New J. Chem.* **2002**, *26*, 1171. (b) Kalinowski, J.; Cocchi, M.; Virgili, D.; Fattori, V.; Williams, J. A. G. *Adv. Mater.* **2007**, *19*, 4000.

spectrum of **13**-12 is virtually unchanged. Apparently, heat treatment of the former results in the formation of a new emitting species, whose lifetime at 600 nm is around 17 ± 3 μs. At shorter wavelengths (ca. 525 nm) an additional, much shorter component of around 5 μs is also observed, suggesting that the lower-energy species can be populated by energy transfer from the higher one. The dramatic effect of heating is observed only for the 100% film; for example, the spectrum of the 90% sample in PC is unchanged on heating. This observation suggests that the formation of the new species must be associated with specific intermolecular interactions, as may be the case for aggregation via orbital overlap. That the molecular organization has changed to give rise to this new emitting species is supported by DSC measurements, which show an endothermic event at 108 °C. As microscopy does not see a major change at this temperature, the event is assigned as a transition between two crystal polymorphs.

Intermolecular organization then clearly has a significant effect on emission characteristics. We have previously reported that the emission wavelength of some disk-like $N,C,N-Pt^{II}$ complexes could be controlled by the manner in which the sample was cooled from the isotropic state,[8] while Kato and co-workers have observed that the nature of the liquid crystal state can determine emission behavior.[9] Thus, the combination of emitter and liquid crystal properties offers control over the nature of the emission via the molecular organization. For the present complexes, the high luminescence efficiency coupled with the potential to align the complexes in the liquid crystal phase promises to yield highly dichroic emission from a system that harvests from singlet and triplet states alike. Results of these studies will be reported in due course.

Experimental Section

New compounds were characterized by ^1H and ^{13}C NMR spectroscopy recorded on JEOL ECX400 or JEOL EX270 spectrometers, while NOE experiments were carried out on a Bruker AV500. Elemental analysis was carried out in house (Exeter Analytical Inc., CE-440 Elemental Analyzer).

Enthalpies of liquid crystal transitions were measured using a Mettler Toledo DSC822^e differential scanning calorimeter, equipped with Mettler Toledo TS0801RO Sample Robot and calibrated against pure indium metal. Heating and cooling rates were 5 or 10 °C min^{-1}. Optical textures were recorded using an Olympus BX50 polarizing microscope equipped with a Linkam scientific LTS350 heating stage, Linkam LNP2 cooling pump, and Linkam TMS92 controller.

All chemicals were used as supplied, unless noted otherwise. The 1,2,4-triazines were synthesized using a very simple route.[6,7] The synthesis is given for one example of each series of molecules, while the principal analytical data are detailed in the Supporting Information, for all ligands and complexes.

Preparation of the Pyridine Ligands. *3,6-Di(4-methoxyphenyl)-1,2,4-triazine* (***3***). 4-Methoxybenzohydrazide (8.74 mmol, 1.45 g), 2-bromo-4′-methoxyacetophenone (4.37 mmol, 1.00 g) and sodium acetate (4.81 mmol, 0.39 g) were added to a solution of ethanol and acetic acid (20 cm^3, 7:3). The mixture was stirred and heated under reflux for 16 h, after which it was cooled slowly. The crystalline precipitate was filtered off and washed with ethanol (10 cm^3) and diethyl ether (10 cm^3) to give a yellow, crystalline solid. Yield 0.97 g (3.32 mmol, 76%).

^1H NMR δ_H (270 MHz, $CDCl_3$): 8.94 (1H, s, H^6), 8.50 (2H, d, J = 8.9 Hz, AA′XX′) 8.09 (8H, d, J = 8.8 Hz, AA′XX′), 7.07 (2H, d, J = 8.8 Hz, AA′XX′), 7.04 (2H, d, J = 8.9 Hz, AA′XX′), 3.89 (3H, s, OCH_3), 3.88 (3H, s, OCH_3).

2,5-Di(4-methoxyphenyl)pyridine (***4***). 3,6-Di(4-methoxyphenyl)-1,2,4-triazine (8.52 mmol, 2.50 g) was added to a solution of bicyclo[2.2.1]hepta-2,5-diene (86.3 mmol, 7.95 g) in 1,2-dichlorobenzene (20 cm^3). The mixture was stirred and heated under reflux for 5 h. During the reaction more bicyclo[2.2.1]hepta-2,5-diene (88.45 mmol, 8.15 g) was added, and the solution was left under reflux overnight, after which it was cooled, the solvent was removed by filtration, and the solid was washed with ethanol (50 cm^3) and ethoxyethane (50 cm^3) to give a gray, crystalline solid. Yield 1.61 g (5.54 mmol, 65%).

^1H NMR δ_H (270 MHz, $CDCl_3$): 8.79 (1H, d, $^4J_{HH}$ = 2.7 Hz, H^6), 7.79 (2H, d, J = 8.9 Hz, AA′XX′), 7.86 (1H, dd, $^3J_{HH}$ = 8.3 Hz, $^4J_{HH}$ = 2.7 Hz, H^4), 7.71 (1H, d, $^3J_{HH}$ = 8.2 Hz, H^3), 7.55 (2H, d, $^3J_{HH}$ = 8.8 Hz, AA′XX′), 6.95 (2H, d, J = 8.9 Hz, AA′XX′), 6.94 (2H, d, J = 8.8 Hz, AA′XX′), 3.85 (3H, s, OCH_3), 3.86 (3H, s, OCH_3).

2,5-Di(4-hydroxyphenyl)pyridine (***5***). 2,5-Di(4-methoxyphenyl)pyridine (3.60 mmol, 1.05 g) was added to molten pyridinium chloride (45.43 mmol, 5.25 g) at 200 °C and stirred for 16 h. After some cooling, the still warm mixture was added to water (50 cm^3) and stirred for 15 min. The resulting solid was recovered by filtration and washed with water (100 cm^3) and propanone (100 cm^3), to give a green solid. Yield 0.56 g (2.14 mmol, 59%)

^1H NMR δ_H (270 MHz, dmso): 10.11 (1, broad s, OH), 9.87 (1H, broad s, OH), 8.86 (1H, d, $^4J_{HH}$ = 1.9 Hz, H^6), 8.53 (1H, dd, $^3J_{HH}$ = 8.7 Hz, $^4J_{HH}$ = 1.9 Hz, H^4), 8.19 (1H, d, $^3J_{HH}$ = 8.7 Hz, H^3), 7.98 (2H, d, $^3J_{HH}$ = 8.7 Hz, Ar), 7.70 (2H, d, $^3J_{HH}$ = 8.6 Hz, Ar), 6.98 (2H, d, $^3J_{HH}$ = 8.7 Hz, Ar), 6.94 (2H, d, $^3J_{HH}$ = 8.6 Hz, Ar).

2,5-Di(4-dodecyloxyphenyl)pyridine (***6***-*12*). 2,5-Di(4-hydroxyphenyl)pyridine (1.90 mmol, 0.50 g) was added to a solution of 1-bromododecane (4.73 mmol, 1.18 g) and potassium carbonate (5.50 mmol, 0.76 g) in DMF (20 cm^3). The solution was stirred and heated at 90 °C for 12 h. Following cooling, the solid was recovered by filtration and washed with water (70 cm^3), propanone (50 cm^3), and chloroform (10 cm^3), to give a colorless, crystalline solid. Yield 0.51 g (0.85 mmol, 45%).

^1H NMR δ_H (270 MHz, $CDCl_3$): 8.79 (1H, d, $^4J_{HH}$ = 2.3 Hz, H^6), 7.90 (2H, d, J = 8.9 Hz, AA′XX′), 7.80 (1H, dd, $^3J_{HH}$ = 8.3 Hz, $^4J_{HH}$ = 2.3 Hz, H^4), 7.64 (1H, d, $^3J_{HH}$ = 8.3 Hz, H^3), 7.48 (2H, d, J = 8.7 Hz, AA′XX′), 6.94 (2H, d, J = 8.9 Hz, AA′XX′), 6.93 (2H, d, J = 8.8 Hz, AA′XX′), 3.94 (4H, m, OCH_2), 1.74 (4H, m, CH_2), 1.41 (4H, m, CH_2), 1.19 (32H, broad m, CH_2), 0.81 (6H, t, Me). HRMS (Supporting Information) (m/z): [MH^+] for $C_{41}H_{62}NO_2$, found (expected) 600.4775 (600.9365).

2,5-Di(4-methoxyphenyl)cyclopentenopyridine (***7***). 3,6-Di(4-methoxyphenyl)-1,2,4-triazine (4.00 mmol, 1.17 g) was added to 1-(*N*-morpholino)cyclopentene (18.8 mmol, 2.88 g). The mixture was stirred and heated under an argon atmosphere, at 190 °C for 2 h. During the reaction more 1-(*N*-morpholino)cyclopentene (6.30 mmol, 0.97 g) was added, and the solution was left for an additional 1 h at 190 °C. After the mixture was cooled, ethanol (10 cm^3) was added. The precipitate was recovered by filtration and the solid washed with ethanol (15 cm^3) to give a colorless, crystalline solid. Yield 0.88 g (2.68 mmol, 67%).

^{1}H NMR δ_H (270 MHz, $CDCl_3$): 8.49 (1H, s, H^6), 7.74 (2H, d, $J = 2.27$ Hz, AA′XX′), 7.41 (2H, d, $J = 2.10$ Hz, AA′XX′), 6.99 (4H, d, $J = 8.8$ Hz, AA′XX′), 3.85 (H, s, OCH_3), 3.14 (2H, t, CH_2 cyclopenteno), 3.01 (2H, t, CH_2 cyclopent), 2.04 (2H, m, CH_2 cyclopent).

2,5-Di(4-hydroxyphenyl)cyclopentenopyridine. 2,5-Di(4-methoxyphenyl)cyclopentenopyridine (3.59 mmol, 1,19 g) was added to molten pyridinium chloride (45.43 mmol, 5.25 g) at 200 °C and stirred for 12 h. When the mixture was still warm, water (50 cm^3) was added and the mixture stirred for 15 min. The solid was recovered by filtration and washed with water (100 cm^3) and propanone (100 cm^3), to give a dark solid. Yield 0.98 g (3.23 mmol, 90%).

^{1}H NMR δ_H (270 MHz, dmso): 10.47 (1H, broad s, OH), 10.05 (1H, broad s, OH), 8.51 (1H, s, H^6), 7.66 (2H, d, $^3J_{HH} = 8.7$ Hz, Ar), 7.47 (2H, d, $^3J_{HH} = 8.6$ Hz, Ar), 6.98 (4H, m, Ar), 3.15 (4H, m, CH_2 cyclopentene), 2.09 (2H, m, CH_2 cyclopentene).

2,5-Di(4-dodecyloxyphenyl)cyclopentenopyridine (***8-12***). 2,5-Di(4-hydroxyphenyl)-cyclopentenopyridine (1.90 mmol, 0.581 g) was added to a solution of 1-bromododecane (4.73 mmol, 1.18 g) and potassium carbonate (5.50 mmol, 0.762 g) in DMF (20 cm^3). The solution was stirred and heated at 90 °C for 12 h. After the mixture was cooled, it was dissolved in water (150 cm^3), filtered off the precipitate, and washed with ethanol (50 cm^3) and propanone (25 cm^3). The crude product was purified by column chromatography (silica gel 10:1 $CHCl_3$/ethyl acetate), the fractions were collected, and the solvent was removed by rotary evaporator to give a brown pale solid. Yield 0.68 g (0.85 mmol, 55%).

^{1}H NMR δ_H (270 MHz, $CDCl_3$): 8.49 (1H, s, H^6), 7.73 (2H, d, $J = 8.7$ Hz, AA′XX′), 7.39 (2H, d, $J = 8.7$ Hz, AA′XX′), 6.98 (4H, d, $J = 8.7$ Hz, AA′XX′), 3.94 (4H, m, OCH_2), 3,14 (2H, t, CH_2 cyclopent), 3.02 (2H, t, CH_2 cyclopent), 2.04 (2H, m, CH_2 cyclopent), 1.80 (4H, m, CH_2), 1.47 (4H, m, CH_2), 1.28 (32H, broad m, CH_2), 0.88 (6H, t, Me). HRMS (Supporting Information) (m/z): [MH^+] for $C_{44}H_{66}NO_2$, found (expected) 640.5088 (641.0003).

Preparation of Platinum complexes. *Complex **9-12***. Potassium tetrachloroplatinate(II) (0.241 mmol, 0.100 g), solubilized in the minimum amount of hot water, was added to a solution of **6**-12 (0.242 mmol, 0.145 g) in acetic acid (50 cm^3). The mixture was stirred and heated under vigorous reflux overnight. The precipitate was recovered by filtration and washed successively with hot acetic acid (30 cm^3), water (60 cm^3), chloroform (50 cm^3), and diethyl ether (30 cm^3). The product was insoluble in the most common NMR solvents and was used in the next step without further purification. Yield 0.094 g (0.057 mmol, 33%).

*Complex **11-12***. Complex **9**-12 (0.060 mmol, 0.100 g) was dissolved in dmso (10 cm^3) and heated under reflux with stirring for 30 min. The solvent was removed by rotary evaporator and the resulting compound purified by short column chromatography on silica, using chloroform as eluant. Yield 0.095 g (0.105 mmol, 87%).

^{1}H NMR δ_H (270 MHz, $CDCl_3$): 9.70 (1H, d, $^4J_{HH} = 2.0$ Hz, $^3J_{HPt} = 36.5$ Hz, H^6), 7.94 (1H, d, $^4J_{HH} = 2.3$ Hz, $^3J_{HPt} = 52.7$ Hz, Ar), 7.87 (1H, dd, $^3J_{HH} = 8.5$ Hz $^4J_{HH} = 2.0$ Hz, H^4), 7.51 (1H, d, $^3J_{HH} = 8.8$ Hz, H^3), 7.46 (2H, d, $J = 8.7$ Hz, AA′XX′), 7.36 (1H, d, $^3J_{HH} = 8.6$ Hz, Ar), 6.91 (2H, d, $J = 8.7$ Hz, AA′XX′), 6.66 (1H, dd, $^3J_{HH} = 8.7$ Hz, $^4J_{HH} = 2.3$ Hz, Ar) 3.95 (4H, m, OCH_2), 3.59 (6H, s, $^3J_{HPt} = 11.0$ Hz, SMe), 1.72 (4H, m, CH_2), 1.39 (4H, m, CH_2), 1.20 (32H, broad m, CH_2), 0.81 (6H, t, Me).

*Complex **13-12***. Complex **11**-12 (0.110 mmol, 0.100 g) was added to a solution of sodium acetylacetonate monohydrate (1.16 mmol, 0.163 g) in propanone (60 cm^3) and stirred at room temperature for 4 h. After the reaction the solvent was removed by rotary evaporator, washed with water (50 cm^3), and crystallized from propanone.

^{1}H NMR δ_H (270 MHz, $CDCl_3$): 9.04 (1H, d, $^4J_{HH} = 2.1$ Hz, $^3J_{HPt} = 35.3$ Hz, H^6), 7.82 (1H, dd, $^3J_{HH} = 8.5$ Hz, $^4J_{HH} = 2.1$ Hz, H^4), 7.45 (2H, d, $J = 8.8$ Hz, AA′XX′) 7.42 (1H, d, $^3J_{HH} = 8.6$ Hz, H^3), 7.39 (1H, d, $^3J_{HH} = 8.6$ Hz, Ar), 7.05 (1H, d, $^4J_{HH} = 2.5$ Hz, $^3J_{HPt} = 39.6$ Hz, Ar), 6.94 (2H, d, $J = 8.8$ Hz, AA′XX′), 6.60 (1H, dd, $^3J_{HH} = 8.5$ Hz, $^4J_{HH} = 2.5$ Hz, Ar), 5.41 (1H, s, CO−CH-CO), 4,00 (2H, t, OCH_2), 3.94 (2H, t, OCH_2), 1.94 (3H, s, −CO−CH_3), 1.93 (3H, s, −CO−CH_3), 1.74 (4H, m, CH_2), 1.40 (4H, m, CH_2), 1.20 (32H, broad m, CH_2), 0.81 (6H, t, Me). MS-FAB (m/z): [M^+] for $C_{46}H_{67}NO_4Pt$, found (expected) 892.47 (892.47).

*Complex **10-12***. Potassium tetrachloroplatinate(II) (0.241 mmol, 0.100 g), solubilized in the minimum amount of hot water, was added to a solution of **8**-12 (0.242 mmol, 0.155 g) in acetic acid (50 cm^3), and the mixture was stirred and heated under reflux overnight. The precipitate was recovered by filtration and washed with water (30 cm^3), ethanol (50 cm^3), and diethyl ether (25 cm^3). The product was insoluble in the most common NMR solvents and was used in the next step without further purification. Yield 0.137 g (0.079 mmol, 47%).

*Complex **12-12***. Complex **10**-12 (0.0575 mmol, 0.100 g) was dissolved in dmso (10 cm3) and heated under reflux with stirring for 30 min. The solvent was removed by rotary evaporator and the resulting compound purified by column chromatography on silica, using chloroform as eluant. Yield 0.101 g (0.105 mmol, 95%).

^{1}H NMR δ_H (270 MHz, $CDCl_3$): 9.45 (1H, s, $^3J_{HPt} = 36.8$ Hz, H^6), 8.04 (1H, d, $^4J_{HH} = 2.6$ Hz, $^3J_{HPt} = 55.1$ Hz, Ar), 7.52 (1H, d, $^3J_{HH} = 8.8$ Hz, Ar) 7.31 (2H, d, $J = 8.7$ Hz, AA′XX′), 6.90 (2H, d, $J = 8.7$ Hz, AA′XX′), 6.67 (1H, dd, $^3J_{HH} = 8.6$ Hz, $^4J_{HH} = 2.5$ Hz, Ar), 3.99 (2H, t, OCH_2), 3.93 (2H, t, OCH_2), 3.59 (6H, s, $^3J_{HPt} = 21.0$ Hz, SMe), 3.29 (2H, t, CH_2 cyclopent), 3.01 (2H, t, CH_2 cyclopent), 2.12 (2H, m, CH_2 cyclopent), 1.74 (4H, m, CH_2), 1.40 (4H, m, CH_2), 1.21 (32H, broad m, CH_2), and 0.82 (6H, t, CH_3).

*Complex **14-12***. Complex **12**-12 (0.11 mmol, 0.100 g) was added to a solution of sodium acetylacetonate monohydrate (0.23 mmol, 0.032 g) in propanone (60 cm^3) and stirred at room temperature for 12 h. After the reaction the solvent was removed by rotary evaporator, and the product was solubilized in CH_2Cl_2 and then filtered. The solvent was removed by rotary evaporator, and the crude product was purified by short column chromatography on silica, using chloroform as eluant. Yield 0.086 g (0.93 mmol, 85%).

^{1}H NMR δ_H (270 MHz, $CDCl_3$): 8.75 (1H, s, $^3J_{HPt} = 33.7$ Hz, H^6), 7.45 (1H, d, $^3J_{HH} = 8.6$ Hz, Ar), 7.30 (2H, d, $J = 8.7$ Hz, AA′XX′), 7.12 (1H, d, $^4J_{HH} = 2.6$ Hz, $^3J_{HPt} = 37.7$ Hz, Ar), 6.92 (2H, d, $J = 8.7$ Hz, AA′XX′), 6.59 (1H, dd, $^3J_{HH} = 8.6$ Hz, $^4J_{HH} = 2.6$ Hz, Ar), 5.38 (1H, s, CO−CH-CO), 4.01 (2H, t, OCH_2), 3.94 (2H, t, OCH_2), 3.30 (2H, t, CH_2 cyclopent), 2.95 (2H, t, CH_2 cyclopent), 2.12 (2H, m, CH_2 cyclopent),1.93 (3H, s, CO−CH_3), 1.88 (3H, s, CO−CH_3), 1.75 (4H, m, CH_2), 1,41 (4H, m, CH_2), 1.20 (32H, broad m, CH_2) and 0.81 (6H, t, CH_3). MS-FAB (m/z): [M^+] for $C_{49}H_{71}NO_4Pt$, found (expected): 932.50 (932.50).

Photophysical Measurements. Absorption spectra in solution were measured on a Biotek Instruments XS spectrometer, using quartz cuvettes of 1 cm path length. Steady-state luminescence spectra were measured using a Jobin Yvon FluoroMax-2 spectrofluorimeter, fitted with a red-sensitive Hamamatsu R928 photomultiplier tube; the spectra shown are corrected for the wavelength dependence of the detector, and the quoted emission

maxima refer to the values after correction. Samples for emission measurements were contained within quartz cuvettes of 1 cm path length modified with appropriate glassware to allow connection to a high-vacuum line. Degassing was achieved via a minimum of three freeze−pump−thaw cycles while connected to the vacuum manifold; final vapor pressure at 77 K was $< 5 \times 10^{-2}$ mbar, as monitored using a Pirani gauge. Luminescence quantum yields were determined using $[Ru(bpy)_3]Cl_2$ in air-equilibrated aqueous solution ($\phi = 0.028$[27]) as the standard; estimated uncertainty in ϕ is ±20% or better. The emission spectra of the films were measured using a Hitachi F-4500 spectrophotometer, and the samples were prepared using a Chemat Technology Spin-Coater KW-4A.

The luminescence lifetimes of the complexes in degassed solution were measured by multichannel scaling following excitation using a μs-pulsed xenon lamp at 400 nm. The emitted light was detected at 90° using a Peltier-cooled R928 PMT after passage through a monochromator. The estimated uncertainty in the quoted lifetimes is ±10% or better. The shorter lifetimes of the model complex [Pt(bpy)(acac)] and those of the new complexes in aerated solution were measured using the same detector operating in time-correlated single-photon-counting mode, by excitation with a laser diode at 374 nm. Bimolecular rate constants for quenching by molecular oxygen, k_Q, were determined from the lifetimes in degassed and air-equilibrated solution, taking the concentration of oxygen in CH_2Cl_2 at 0.21 atm O_2 to be 2.2 mmol dm^{-3}.[28] The luminescence lifetimes of the films were measured using the same system.

Supporting Information Available: Crystallographic information (CIF) and NMR characterization, planarity of coordination center and torsion angles, Pt−Pt distances and selected ligand−Pt−Pt angles, analytical data, photomicrographs, and normalized absorption spectra (PDF). This material is available free of charge via the Internet at http://pubs.acs.org.

(27) Nakamaru, K. *Bull. Chem. Soc. Jpn.* **1982**, *55*, 2697.
(28) Murov, S. L.; Carmichael, I.; Hug, G. L. *Handbook of Photochemistry*, 2nd ed.; Marcel Dekker: New York, 1993.